

One-dimensional Van Hove polaritons

K. B. Arnardottir,^{1,2} O. Kyriienko,^{1,3} M. E. Portnoi,^{4,5} and I. A. Shelykh^{1,3}

¹*Science Institute, University of Iceland, Dunhagi-3, IS-107, Reykjavik, Iceland*

²*Fysikum, Stockholms Universitet, S-106 91 Stockholm, Sweden*

³*Division of Physics and Applied Physics, Nanyang Technological University 637371, Singapore*

⁴*School of Physics, University of Exeter, Stocker Road, Exeter EX4 4QL, United Kingdom*

⁵*International Institute of Physics, Avenida Odilon Gomes de Lima, 1722,*

Capim Macio, Código de Endereçamento Postal: 59078-400, Natal - RN, Brazil

(Dated: January 12, 2021)

We study the light-matter coupling of microcavity photons and an interband transition in a one-dimensional (1D) nanowire. Due to the Van Hove singularity in the density of states, resulting in a resonant character of the absorption line, the achievement of strong coupling becomes possible even without the formation of a bound state of an electron and a hole. The calculated absorption in the system and corresponding energy spectrum reveal anti-crossing behavior characteristic of the formation of polariton modes. In contrast to the case of conventional exciton polaritons, the formation of 1D Van Hove polaritons will not be restricted to low temperatures and can be realized in any system with a singularity in the density of states.

I. INTRODUCTION

Light-matter coupling is an area of research emerging at the boundary between condensed matter physics and optics which has both fundamental and applied dimensions. The possibility of reaching the regime of strong coupling, for which confined cavity photons and matter excitations are strongly mixed, is of particular interest.¹ In this situation a new type of elementary excitations, known as polaritons, appear in the system. Having a hybrid nature, they combine the properties of both light and matter. Several geometries have been proposed for the realization of the strong coupling regime.

The interaction of a cavity photon mode with a two-level system which mimics optical transitions in an individual atom or single quantum dot (QD) is the origin of cavity quantum electrodynamics (cavity QED).^{2,3} One should note that the achievement of strong coupling in such a system is a non-trivial task due to a rather small light-matter interaction constant. However, recent advances in nanotechnology have led to the possibility of creating high-finesse optical cavities and have resulted in the observation of Rabi doublets and Mollow triplets in the emission spectrum of individual QDs.⁴⁻⁶ Moreover, the strong coupling of a single photon to a superconducting qubit, which has a two-level structure as well, has been demonstrated in a radio-wave superconducting cavity.⁷

To increase light-matter coupling, quantum wells (QWs) can be used instead of individual QDs. In this case, coupling occurs between a two-dimensional (2D) QW exciton, associated with a sharp absorption peak slightly below the bandgap energy, and a photonic mode of a planar cavity tuned in resonance with it. Observed for the first time two decades ago,⁸ exciton-polariton physics is now experiencing increased interest connected to the possible realization of polariton lasing with an extremely low threshold,⁹ and the achievement of Bose-Einstein condensates¹⁰ (BECs), and su-

perfluid states¹¹ for temperatures much higher than for atomic systems^{12,13} and cold excitons in solids.¹⁴ This is a consequence of the small effective mass of polaritons which allows a pronounced manifestation of quantum collective phenomena for a critical temperature around 20 K in CdTe structures¹⁰ and even at room temperatures in wide-band-gap materials with large exciton binding energy and strong light-matter interaction (GaN, ZnO).^{15,16} Additionally, polaritons have been proposed as basic ingredients for spinoptronic devices¹⁷ and all-optical logical elements and integrated circuits.^{18,19}

While most attention in the field of exciton polaritons is drawn to two-dimensional structures, the strong light-matter interaction of excitons in one-dimensional nanowires with a confined cavity mode has also been studied.^{20,21} Their properties were shown to be improved over the exciton-polaritons analogs in the quantum wells due to their larger exciton binding energy.²¹ However, the physics of light matter coupling remains essentially the same.

Another system where strong light-matter coupling was experimentally achieved is the intersubband transitions in quantum wells. It was shown by Dini and co-workers²² that the absorption of intersubband resonance placed into a cavity reveals the characteristic anti-crossing behavior. The attractive peculiarity of such a system in comparison to those based on conventional interband exciton-polaritons is a non-vanishing ratio of the Rabi frequency to the transition energy, which enables an exploration of the ultra-strong-coupling regime.²³ In addition, unlike interband transitions in a 2D system, strong electron-hole interactions and the formation of excitons are not necessary for obtaining the strong coupling regime,²⁴ although they play a certain role in structures with highly doped QWs, where the formation of intersubband plasmon-polaritons^{26,27} and Fermi edge polaritons²⁸ can be observed.

For any experimental geometry, the main condition which must be satisfied to drive the system into strong

coupling is the presence of a narrow resonance in its photoabsorption spectrum. Mathematically, this condition reads

$$g = \frac{\hbar\Omega_R}{2} \gg \gamma_{cav} - \gamma_{ex}, \quad (1)$$

where g denotes the light-matter coupling strength, Ω_R is the corresponding Rabi frequency (the light-matter interaction constant), γ_{cav} is the damping constant of the cavity mode and γ_{ex} is the width of the absorption resonance.^{1,25} In 2D interband absorption this condition requires strong exciton-hole attraction resulting in the formation of an exciton. However, in the 1D case this is not strictly speaking necessary, since the behavior of the density of states $\rho(E)$ in 2D and 1D is qualitatively different. In the former case, the density of states is constant, while in the latter it diverges around the points E_0 at which the energy as a function of the momentum k reaches its minimum,

$$\rho(E) \sim \frac{1}{\sqrt{E - E_0}}. \quad (2)$$

This peculiarity, known as a Van Hove singularity, makes the optical properties of 1D nanostructures different from those of the bulk and 2D cases and leads to the resonant character of photoabsorption even without any excitonic effects.

In this article we analyze the possibility of the realization of the strong-coupling regime between a cavity photon and the interband transition of a one-dimensional nanowire driven by the presence of the Van Hove singularity in the 1D density of states. We consider the case of the cavity mode tuned to the interband transition, while the 1D exciton is detuned far from the resonance and thus does not affect the properties of the system in the frequency range we consider. The demonstrated spectrum of the elementary excitation reveals anti-crossing behavior characteristic of the formation of polaritonic modes for realistic cavity quality factors. We show that this effect is robust against both finite temperature and interaction corrections.

II. MODEL

We consider a system consisting of a 1D semiconductor wire embedded in an optical microcavity, which is tuned into resonance with a direct interband transition (see the sketch in Fig. 1).

To calculate the optical response of the coupled wire-resonator system, we use an approach based on Green's function technique. Information about the dispersion of elementary excitations in the coupled quantum-wire-cavity system can be extracted from the poles of the Green's function of the cavity photon interacting with the interband transition $D(q, \omega)$. The absorption spectrum can be determined from the polarization operator $\Pi(q, \omega)$. The formalism we are going to use is analogous

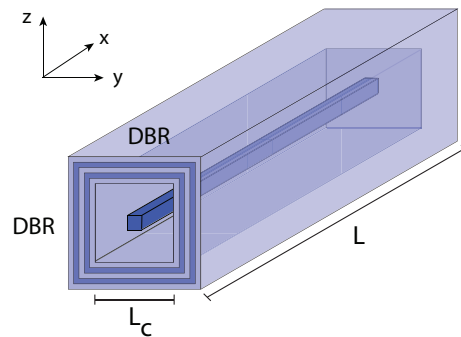


FIG. 1: (Color online) Sketch of the system. A semiconductor microcavity is formed with two pairs of distributed Bragg reflectors (DBRs) with the cavity width in the z and y direction being L_c . The length of the 1D semiconductor wire is L .

to that developed in Ref. [27] for intersubband transitions.

We start with a calculation of the polarization operator, accounting for the possibility of multiple re-emissions and re-absorptions of a cavity photon by the interband transition in the quantum wire. These processes can be represented graphically as an infinite set of diagrams shown in Fig. 2(a), which can be reduced to the Dyson equation shown in Fig. 2(b). These series diagrammatically describe the strong light-matter coupling regime, where multiple interaction with the cavity mode renormalizes the overall absorption in the system. The corresponding solution of the Dyson equation reads

$$\Pi(q, \omega) = \frac{\Pi_0(q, \omega)}{1 - g^2 D_0(q, \omega) \Pi_0(q, \omega)}, \quad (3)$$

where Π_0 denotes the interband polarization operator depicting excited electron-hole pair in the conduction and valence bands and g stands for the light-matter interaction constant. D_0 is a propagator of the cavity photon, given by²⁷

$$D_0(q, \omega) = \frac{2\hbar\omega_{cav}(q)}{\hbar\omega^2 - \hbar\omega_{cav}^2(q) + 2i\gamma_{cav}\hbar\omega_{cav}(q)}, \quad (4)$$

with $\gamma_{cav} = \hbar/\tau_{ph}$ representing the damping of the cavity mode appearing due to the imperfectness of the cavity, where τ_{ph} is the cavity photon lifetime. $\hbar\omega_{cav}$ denotes the dispersion of the cavity photon and can be written as

$$\hbar\omega_{cav}(q) = \frac{\hbar c}{n} |\mathbf{q}| = \frac{\hbar c}{n} \sqrt{q_x^2 + q_y^2 + q_z^2}, \quad (5)$$

where n is the refractive index of the cavity and c denotes the speed of light. The confinement in the y and z directions leads to a quantization of the photon momentum components q_y and q_z , while it can freely propagate in the x direction. Here we are interested in the photonic mode with the lowest energy which corresponds to the single antinode lying in the center of the cavity. The dispersion of the cavity photon as a function of q_x (in the

following we denote it as q for simplicity) reads:

$$\begin{aligned} \hbar\omega_{cav}(q) &= \frac{\hbar c}{n} \sqrt{q^2 + \left(\frac{\pi}{L_c}\right)^2 + \left(\frac{\pi}{L_c}\right)^2} \approx \frac{c\hbar L_c}{2\sqrt{2}\pi n} q^2 \\ &+ \frac{\sqrt{2}\pi c\hbar}{nL_c} \equiv \frac{\hbar^2 q^2}{2m_{ph}} + E_g + \delta, \end{aligned} \quad (6)$$

where m_{ph} is the effective mass of the photon and δ is the detuning between the cavity mode and the bandgap E_g .

The interband polarization operator Π_0 used in Eq. (3) describes the absorption of the wire in the absence of the cavity. Strictly speaking, its calculation requires a full account of the many-body interactions in the system and thus represents a formidable problem. In the current work, however, we are interested in the effects of the Van Hove singularity only, and as a first approximation we consider non-interacting particles. However, in the later discussion we will account for Coulomb interactions using the random phase approximation (RPA) and compare the results with those of the non-interacting case. The bare interband polarization operator $\Pi_0(q, \omega)$ is represented by a ‘‘bubble’’ diagram and can be calculated as

$$\begin{aligned} i\Pi_0(q, \omega) &= - \int \frac{dk}{2\pi/L} \frac{d\nu}{2\pi/\hbar} [iG_e(k+q, \nu+\omega) iG_h(k, \nu) \\ &+ iG_h(k+q, \nu+\omega) iG_e(k, \nu)]. \end{aligned} \quad (7)$$

Here $G_e(q, \omega)$ and $G_h(q, \omega)$ are the Green’s functions of an electron in the conduction band and a hole in the valence band, respectively,

$$G_e(q, \omega) = \frac{1}{\hbar\omega - E_g - \hbar^2 q^2 / 2m_e + i\delta}, \quad (8)$$

$$G_h(q, \omega) = \frac{1}{\hbar\omega + \hbar^2 q^2 / 2m_h - i\delta}, \quad (9)$$

where m_e and m_h are the effective electron and hole masses (both taken to be positive), and δ is an infinitesimal parameter. For the case of zero temperature an analytical integration of Eq. (7) can be performed, which leads to an explicit expression for the bare polarization operator Π_0 :

$$\begin{aligned} \Pi_0(q, \omega) &= \frac{L\sqrt{2}\mu}{\hbar} \left(\frac{f_1(q, \omega)}{\sqrt{\hbar\omega + E_g + \hbar^2 q^2 / M - i\gamma_{ex}}} - \right. \\ &\left. - \frac{if_2(q, \omega)}{\sqrt{\hbar\omega - E_g - \hbar^2 q^2 / M + i\gamma_{ex}}} \right), \end{aligned} \quad (10)$$

where μ denotes the reduced mass, $\mu^{-1} = m_e^{-1} + m_h^{-1}$, $M = m_e + m_h$ and L is the length of the wire. The

functions $f_1(q, \omega)$ and $f_2(q, \omega)$ are given by

$$\begin{aligned} f_1(q, \omega) &= \frac{1}{\pi} \left[\tan^{-1} \left(\frac{\pi/a + \beta_e q}{\sqrt{2\mu(\hbar\omega + E_g + \hbar^2 q^2 / M - i\gamma_{ex})}} \right) \right. \\ &\left. + \tan^{-1} \left(\frac{\pi/a - \beta_e q}{\sqrt{2\mu(\hbar\omega + E_g + \hbar^2 q^2 / M - i\gamma_{ex})}} \right) \right], \quad (11) \\ f_2(q, \omega) &= \frac{i}{\pi} \left[\tanh^{-1} \left(\frac{\pi/a + \beta_h q}{\sqrt{2\mu(\hbar\omega - E_g - \hbar^2 q^2 / M + i\gamma_{ex})}} \right) \right. \\ &\left. + \tanh^{-1} \left(\frac{\pi/a - \beta_h q}{\sqrt{2\mu(\hbar\omega - E_g - \hbar^2 q^2 / M + i\gamma_{ex})}} \right) \right], \quad (12) \end{aligned}$$

where we introduced the notations $\beta_e = m_e/M$ and $\beta_h = m_h/M$ and γ_{ex} denotes the non-radiative lifetime of the excitation. The parameter a defines the cut-off of the integration at $\pm\pi/a$ and is proportional to the size of the elementary cell of the material of the wire. For small momentum q , the functions are close to unity in all frequency ranges.

The light-matter coupling constant g can be estimated as²⁹

$$g = |d_{cv}| \sqrt{\frac{\hbar\omega_{cav}}{2\epsilon\epsilon_0 V}} \approx \sqrt{\frac{\hbar^2 e^2}{\epsilon\epsilon_0 \mu L_c^2 L}}, \quad (13)$$

where ϵ and $V = L_c^2 L$ are the dielectric permittivity and the volume of the cavity, respectively, and the cavity length parameters L_c and L are shown in the geometry sketch (Fig. 1). Note that $\Pi_0 \sim L$ and $g \sim L^{-1/2}$, and the observable quantities do not depend on the length of the system L .

The polarization operator Π_0 has both real and imaginary parts, and the latter is related to the absorption coefficient of the electron-hole interband excitation:²⁹

$$\alpha(\omega) = \frac{4\pi\omega}{nc} \chi''(\omega) \sim \text{Im}\Pi_0(q, \omega), \quad (14)$$

where $\chi''(\omega)$ is the imaginary part of the optical susceptibility.

The dispersion of the elementary excitations of the coupled quantum-wire-cavity system can be found from the poles of the renormalized Green function of the cavity photon, accounting for the light-matter coupling $D(q, \omega)$. The corresponding Dyson equation is shown in diagrammatic form in Fig. 2(c). Its solution gives

$$D(q, \omega) = \frac{D_0(q, \omega)}{1 - g^2 D_0(q, \omega) \Pi_0(q, \omega)}, \quad (15)$$

and the equation for the new eigenenergies of the system reads

$$1 - g^2 D_0(q, \omega) \Pi_0(q, \omega) = 0. \quad (16)$$

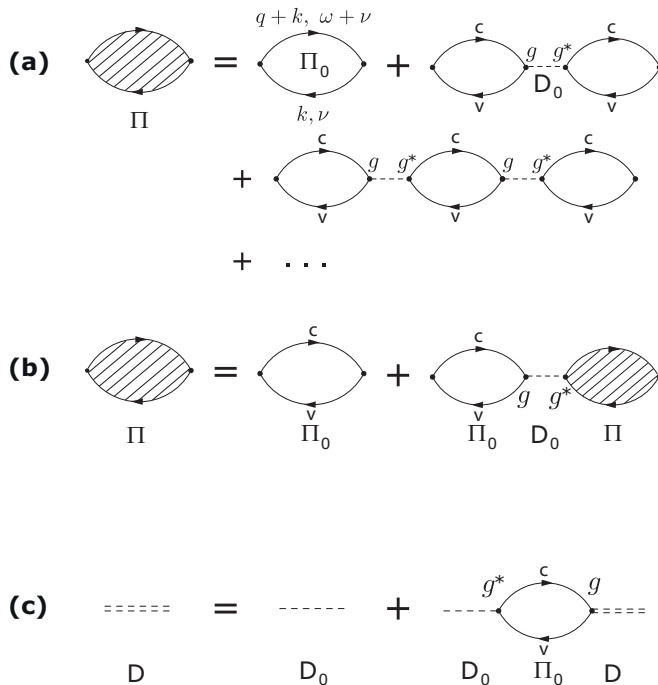


FIG. 2: (a) Feynman diagrams corresponding to the renormalized polarization operator Π , written as a sum of diagrams accounting for processes of multiple re-emissions and re-absorptions. c and v stand for the conduction and valence bands, respectively. (b) Dyson equation for the operator $\Pi(q, \omega)$. The vertex g of the bubble diagrams denotes the coupling constant between the cavity photon and the interband excitation and the dashed line corresponds to the bare cavity photon Green's function D_0 . (c) Dyson equation for the photon Green's function D , represented by a double dashed line, accounting for light-matter coupling.

III. RESULTS

We calculate the renormalized polarization operator of the cavity-excitation system using Eq. (3), and find the energy spectrum of the new modes. The absorption spectrum is calculated from the imaginary part of Π using Eq. (14), while the dispersion relations are extracted from Eq. (16). We used standard parameters for a GaAs sample in our calculations.

Figure 3 shows the absorption spectrum of the coupled GaAs quantum-wire-cavity system and the dispersion relation of the emergent polaritonic modes. The lifetime of the cavity photon was taken as $\tau_{ph} = 10$ ps and the detuning of the cavity mode is $\delta = -10$ meV. One can clearly see the anticrossing of the eigenmodes, characteristic of the strong-coupling regime. The value of the Rabi splitting for parameters considered here is about $\hbar\Omega_R = 1.7$ meV for a single quantum wire embedded in a microcavity. The formation of polaritons is also revealed by a double peak structure of the absorption spectrum shown in Fig. 3(a).

The Rabi splitting can be enhanced by placing more

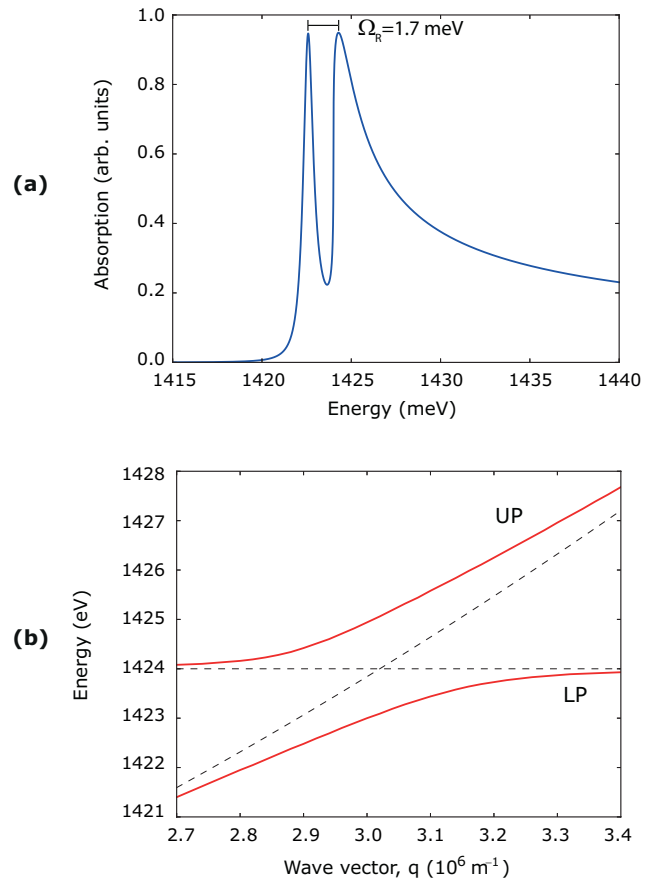


FIG. 3: (Color online) (a) An absorption plot showing polariton states formed by a microcavity photon and interband excitation in a 1D nanowire plotted for the q corresponding to the anticrossing point. (b) The dispersion of elementary excitations in the system. Both plots are for one quantum wire and a photon lifetime of $\tau_{ph} = 10$ ps, which corresponds to $\gamma_{cav} = 0.4$ meV. These parameters yield a Rabi energy of $\hbar\Omega_R = 1.7$ meV.

than one wire in the cavity. In this case the polarization operator corresponding to a single wire, Π_0 , should be replaced by $N_{QW}\Pi_0$, where N_{QW} is the number of wires in the cavity. The decrease of the quality of the cavity, corresponding to the increase of the cavity mode broadening γ_{cav} , results in quenching of the Rabi splitting. The corresponding dependence for different values of N_{QW} is shown in Fig. 4. The damping constant γ_{cav} scales from 0.1 to 10 meV on a logarithmic scale which corresponds to lifetimes spanning from 40 to 0.4 ps, which are possible to realize experimentally.

One can see that for $\gamma_{cav} \gtrsim 1$ meV, which corresponds to a typical quality factor of semiconductor cavities, more than one wire is required for reaching the strong-coupling regime. However, with recent improvement in nanotechnology, fabrication of high-quality resonators with $\gamma_{cav} \sim 0.1$ meV becomes possible.³⁰ This in principle can allow the achievement of strong coupling for an individual wire.

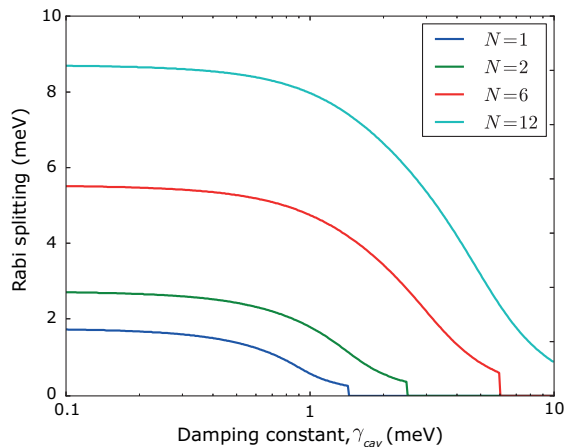


FIG. 4: (Color online) The Rabi splitting as a function of the cavity photon damping constant γ_{cav} plotted for different numbers of quantum wires N embedded in a semiconductor microcavity.

IV. GEOMETRIC, FINITE-TEMPERATURE AND COULOMB CORRECTIONS

In the previous section we considered an idealized situation corresponding to the case of zero temperature, neglecting many-body effects and the placement of all the wires in the antinode of the electric field of the cavity mode. In this section we consider how deviations from these conditions affect the result.

Position of the wires. Strictly speaking, the $\sqrt{N_{QW}}$ enhancement of the Rabi splitting is valid only for very thin wires placed exactly at the antinode of the cavity. For realistic systems we can calculate the Rabi splitting for an array of quantum wires, accounting for the cavity mode structure. For a single quantum wire placed in the center of a microcavity the Rabi frequency is equal to $g = \hbar\Omega_R^{max}$. The index *max* means that the value of the electric field is maximal in the center of the cavity (the antinode for a $\lambda/2$ cavity). However, for a square cavity it changes with deviation from the antinode position as

$$\Omega_R(x) = \Omega_R^{max} \cos(\pi x/L_c) \cos(\pi y/L_c). \quad (17)$$

We can estimate the generalized Rabi splitting for an array of nanowires as

$$\Omega_R^\Sigma = \sqrt{\sum_{i=1}^N \Omega_{R,i}}, \quad (18)$$

where $\Omega_{R,i}$ denotes the Rabi energy for each quantum wire.

We calculate Ω_R^Σ for $N_{QW} = 9$ quantum wires for the geometry sketched in Fig. 5(a). The diameter of the quantum wire is chosen as $L_x^{QW} = 10$ nm with 15 nm separation, and the GaAs cavity width is $L_c = 400$ nm. The result gives $\Omega_R^\Sigma = 2.97\Omega_R^{max}$, which deviates by several percent only from the simple estimation $\Omega_R^\Sigma = \sqrt{N_{QW}}\Omega_R^{max}$.

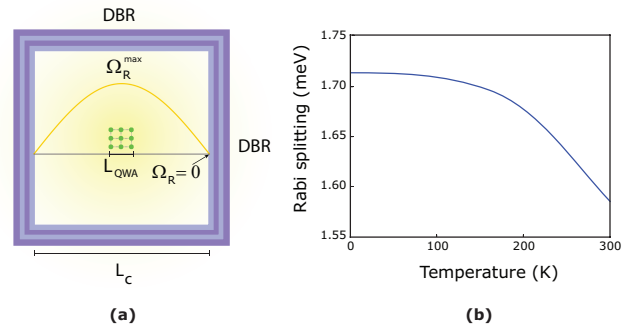


FIG. 5: (Color online) (a) Sketch of the quantum wire array (QWA) embedded in a cavity. The yellow line shows the behavior of the Rabi energy as a function of the confinement direction x . (b) Dependence of the Rabi splitting on temperature calculated for $\gamma_{cav} = 0.4$ meV.

Finite temperature. To account for the finite temperature of the system one can use the Matsubara representation of Green's functions written in imaginary time.³¹ The bare interband polarization operator Π_0 , accounting for temperature effects, can be written as²⁹

$$\Pi_0(0, \omega) = 2 \int \frac{dk}{(2\pi/L)} (f_{v,k} - f_{c,k}) \left[\frac{1}{\hbar\omega - E_g - \frac{\hbar^2 k^2}{2\mu} + i\gamma_{ex}} \right. \quad (19)$$

$$\left. - \frac{1}{\hbar\omega + E_g + \frac{\hbar^2 k^2}{2\mu} - i\gamma_{ex}} \right], \quad (20)$$

where $f_{v,k}$ and $f_{c,k}$ are the Fermi distribution functions for the valence and conduction band, respectively. Here for simplicity we account only for vertical transitions ($q \rightarrow 0$) and perform numerical integration on the momentum k . The Rabi frequency can then be calculated as in the zero temperature case and is plotted as a function of the temperature in Fig. 5(b). One can see that with increasing temperatures up to room temperature the Rabi frequency decreases only slightly. The system remains in the strong light-matter coupling regime and 1D Van Hove polaritons are still observable. A similar situation holds for intersubband polaritons.²²

Coulomb corrections. Previously we restricted our considerations to the non-interacting case. However, in real systems Coulomb interactions do play a role and can change the spectrum of elementary excitations in the system. Accounting for all possible interactions is an extremely complicated task and usually can be done only within certain approximations. For instance, accounting for excitonic resonances requires the use of the ladder approximation.³² It leads to an integral Bethe-Salpeter equation and represents a formidable problem in itself. We do not address this problem in the present work, assuming that the exciton transition lies far from the bare interband transition and thus does not affect the optical properties of the system in the frequency range we consider.

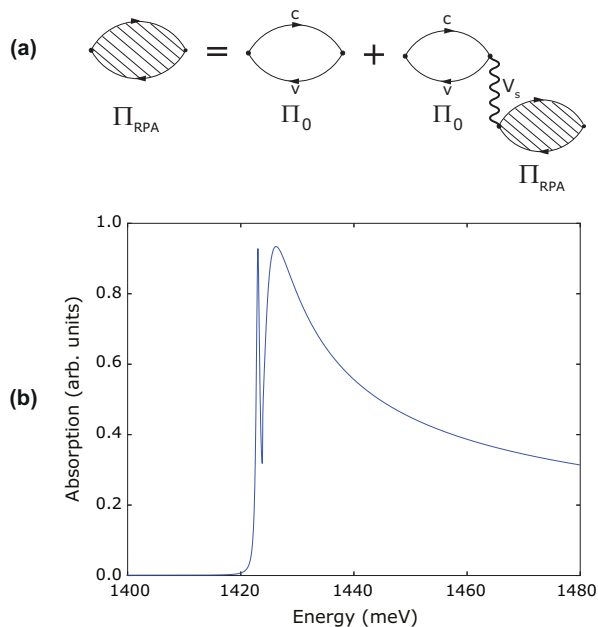


FIG. 6: (a) Feynman diagrams corresponding to RPA corrections to the polarization operator. The thick wiggly line V_S corresponds to the screened Coulomb interaction. (b) Absorption spectrum of the cavity-wire system with Coulomb corrections taken into account using the RPA.

To estimate the influence of the Coulomb corrections we use the RPA approximation^{32,33} shown in diagrammatic form in Fig. 6(a). The resulting equation for the renormalized interband polarization operator is given by

$$\Pi_{RPA} = \frac{\Pi_0}{1 - V_S \Pi_0}, \quad (21)$$

where V_S denotes the screened Coulomb interaction calculated in Ref. [33]. Following the same procedure as before, we substitute for the interband polarization operator Π_0 a modified one, Π_{RPA} , and find that Coulomb corrections in the random phase approximation lead to a broadening and a slight shift of the Van Hove singularity peak. However, the system remains in the strong coupling regime, as can clearly be seen in Fig. 6(b).

Finally, we should note that semiconductor quantum wires can be replaced by carbon nanotubes, which are commonly synthesized in bundles³⁴ or can be arranged in well-aligned arrays.³⁵ In general, excitonic effects are very important in semiconducting carbon nanotubes, as the presence of strongly bound dark excitons results in lumi-

nescence suppression.³⁶ However, tuning the cavity mode to the nanotube's Van Hove singularity should significantly improve light-matter coupling. In quasi-metallic nanotubes with small curvature-induced band gaps and in metallic (armchair) nanotubes with magnetic-field-induced gaps, excitonic effects can be neglected;³⁷ so that our theory of Van Hove polaritons becomes directly applicable. Narrow-gap carbon nanotubes have recently attracted significant attention as promising candidates for terahertz applications.^{38–40} Metallic nanotubes with magnetic-field-induced gaps are of a particular interest, since their spectra can be easily tuned by an external magnetic field. Their similarity to a two-level system is further enhanced by the fast decrease of the dipole transition matrix element away from the field-induced band gap.⁴¹ Another system, for which the developed theory is highly relevant is a bulk semiconductor with Van Hove singularities resulting from quasi-one-dimensional motion along a quantizing magnetic field. Carbon nanotubes in microcavities in both the optical and terahertz frequency ranges as well as bulk materials with magnetic-field-induced Van Hove singularities are subjects of our future work.

V. CONCLUSIONS

In conclusion, we have studied the light-matter coupling of a microcavity photon and an interband transition in a 1D nanowire. Due to the resonant character of the absorption spectrum provided by the Van Hove singularity of the 1D density of states, the achievement of the strong coupling regime becomes possible even in the absence of excitonic effects. We have calculated the dispersions of the resulting polariton modes and the absorption spectra of the coupled wire-cavity system for realistic values of parameters. We have examined the influence of Coulomb corrections and have shown that 1D Van Hove polaritons are robust against temperature changes and can exist even at room temperature.

Acknowledgments

This work was supported by the EU FP7 ITN Spin-Optronics (Grant No. 237252) and the FP7 IRSES projects SPINMET (Grant No. 246784) and QOCaN (Grant No. 316432). O. K. acknowledges support from the Eimskip Fund.

¹ A. V. Kavokin, J. J. Baumberg, G. Malpuech, and F. P. Laussy, *Microcavities* (Oxford University Press, Oxford, 2007).

² S.M. Dutra, *Cavity Quantum Electrodynamics* (Wiley, Hoboken, NJ, 2005).

³ H. Walther, B. T. H. Varcoe, B.-G. Englert, and T. Becker, *Rep. Prog. Phys.* **69** 1325 (2006).

⁴ F. P. Laussy, E. del Valle, and C. Tejedor, *Phys. Rev. Lett.* **101**, 083601 (2008).

⁵ J. P. Reithmaier, G. Şek, A. Löffler, C. Hofmann, S. Kuhn,

- S. Reitzenstein, L. V. Keldysh, V. D. Kulakovskii, T. L. Reinecke, and A. Forchel, *Nature (London)* **432**, 197 (2004).
- ⁶ S. Münch, S. Reitzenstein, P. Franeck, A. Löffler, T. Heindel, S. Höfling, L. Worschech, and A. Forchel, *Opt. Express* **17**, 12821 (2009).
 - ⁷ A. Wallraff, D. I. Schuster, A. Blais, L. Frunzio, R.-S. Huang, J. Majer, S. Kumar, S. M. Girvin, and R. J. Schoelkopf, *Nature (London)* **431**, 162 (2004).
 - ⁸ C. Weisbuch, M. Nishioka, A. Ishikawa and Y. Arakawa, *Phys. Rev. Lett.* **69**, 3314 (1992).
 - ⁹ A. Imamoglu, R. J. Ram, S. Pau and Y. Yamamoto, *Phys. Rev. A* **53**, 4250 (1996).
 - ¹⁰ J. Kasprzak, M. Richard, S. Kundermann, A. Baas, P. Jeambrun, J. M. J. Keeling, F. M. Marchetti, M. H. Szymańska, R. André, J. L. Staehli, V. Savona, P. B. Littlewood, B. Deveaud, and Le Si Dang, *Nature (London)* **443**, 409 (2006).
 - ¹¹ A. Amo, D. Sanvitto, F. P. Laussy, D. Ballarini, E. del Valle, M. D. Martin, A. Lemaître, J. Bloch, D. N. Krizhanovskii, M. S. Skolnick, C. Tejedor, and L. Viña, *Nature (London)* **457**, 291 (2009).
 - ¹² M. H. Anderson, J. R. Ensher, M. R. Matthews, C. E. Wieman, and E. A. Cornell, *Science* **269**, 198 (1995).
 - ¹³ K. B. Davis, M.-O. Mewes, M. R. Andrews, N. J. van Druten, D. S. Durfee, D. M. Kurn, and W. Ketterle, *Phys. Rev. Lett.* **75**, 3969 (1995).
 - ¹⁴ A. A. High, J. R. Leonard, A. T. Hammack, M. M. Fogler, L. V. Butov, A. V. Kavokin, K. L. Campman, and A. C. Gossard, *Nature (London)* **483**, 584 (2012).
 - ¹⁵ J. J. Baumberg, A. V. Kavokin, S. Christopoulos, A. J. D. Grundy, R. Butté, G. Christmann, D. D. Solnyshkov, G. Malpuech, G. Baldassarri Höger von Högersthal, E. Feltn, J.-F. Carlin, and N. Grandjean, *Phys. Rev. Lett.* **101**, 136409 (2008).
 - ¹⁶ S. Christopoulos, G. Baldassarri Höger von Högersthal, A. Grundy, P. G. Lagoudakis, A. V. Kavokin, J. J. Baumberg, G. Christmann, R. Butté, E. Feltn, J.-F. Carlin, and N. Grandjean, *Phys. Rev Lett.* **98**, 126405 (2007).
 - ¹⁷ T. C. H. Liew, I. A. Shelykh, and G. Malpuech, *Physica E* **43**, 1543 (2011).
 - ¹⁸ T. C. H. Liew, A. V. Kavokin and I. A. Shelykh, *Phys. Rev. Lett.* **101**, 016402 (2008).
 - ¹⁹ T. C. H. Liew, A. V. Kavokin, T. Ostatnický, M. Kaliteevski, I. A. Shelykh and R. A. Abram, *Phys. Rev. B* **82**, 033302 (2010).
 - ²⁰ M. A. Kaliteevski, S. Brand, R. A. Abram, V. V. Nikolaev, M. V. Maximov, N. N. Ledentsov, C. M. Sotomayor Torres, A. V. Kavokin, *Phys. Rev. B* **61**, 13791 (2000).
 - ²¹ S. Zhang, W. Xie, H. Dong, L. Sun, Y. Ling, J. Lu, Yu Duan, W. Shen, X. Shen, and Z. Chen, *Appl. Phys. Lett.* **100**, 101912 (2012).
 - ²² D. Dini, R. Kohler, A. Tredicucci, G. Biasiol, and L. Sorba, *Phys. Rev. Lett.* **90**, 116401 (2003).
 - ²³ Y. Todorov, A. M. Andrews, R. Colombelli, S. De Liberato, C. Ciuti, P. Klang, G. Strasser, and C. Sirtori, *Phys. Rev. Lett.* **105**, 196402 (2010).
 - ²⁴ S. De Liberato and C. Ciuti, *Phys. Rev. B* **77**, 155321 (2008).
 - ²⁵ H. Deng, H. Haug, and Y. Yamamoto, *Rev. Mod. Phys.* **82**, 1489 (2010).
 - ²⁶ M. Geiser, F. Castellano, G. Scalari, M. Beck, L. Nevou, J. Faist, *Phys. Rev. Lett.* **108**, 106402 (2012).
 - ²⁷ O. Kyriienko and I. A. Shelykh, *J. Nanophoton.* **6**, 061804 (2012) (see also O. Kyriienko and I. A. Shelykh, arXiv:1112.0240).
 - ²⁸ N. S. Averkiev and M. M. Glazov, *Phys. Rev. B* **76**, 045320 (2007).
 - ²⁹ H. Haug and S. W. Koch, *Quantum Theory of the Optical and Electronic properties of Semiconductors* (World Scientific, Singapore, 1990).
 - ³⁰ E. Wertz, L. Ferrier, D. D. Solnyshkov, R. Johné, D. Sanvitto, A. Lemaître, I. Sagnes, R. Grousson, A. V. Kavokin, P. Senellart, G. Malpuech, and J. Bloch, *Nature Phys.* **6**, 860 (2010).
 - ³¹ H. Bruus and K. Flensberg, *Many-body Quantum Theory in Condensed Matter Physics* (Oxford University Press, Oxford, 2004).
 - ³² S. Das Sarma and D.-W. Wang, *Phys. Rev. Lett.* **83**, 816 (1999).
 - ³³ S. Das Sarma and E. H. Hwang, *Phys. Rev. B* **54**, 1936 (1996).
 - ³⁴ A. Thess, R. Lee, P. Nikalaev, H. Dai, P. Petit, J. Robert, C. Xu, Y. H. Lee, S. G. Kim, A. G. Rinzler, D. T. Colbert, G. E. Scuseria, D. Tomanek, J. E. Fischer, and R. E. Smalley, *Science* **273**, 483 (1996).
 - ³⁵ B. Wang, Y. Ma, N. Li, Y. Wu, F. Li, and Y. Chen, *Adv. Mater.* **22**, 3067 (2010).
 - ³⁶ J. Shaver and J. Kono, *Laser & Photon. Rev.* **1**, 260 (2007).
 - ³⁷ R. R. Hartmann, I. A. Shelykh, and M. E. Portnoi, *Phys. Rev. B* **84**, 035437 (2011).
 - ³⁸ O. V. Kibis, M. Rosenau da Costa, and M. E. Portnoi, *Nano Lett.* **7**, 3414 (2007).
 - ³⁹ M. E. Portnoi, O. V. Kibis, and M. Rosenau da Costa, *Superlattices Microstruct.* **43**, 399 (2008).
 - ⁴⁰ K. G. Batrakov, O. V. Kibis, P. P. Kuzhir, M. R. da Costa, M. E. Portnoi, *J. Nanophoton.* **4**, 041665 (2010).
 - ⁴¹ M. E. Portnoi, M. Rosenau da Costa, O. V. Kibis, and I. A. Shelykh, *Int. J. Mod. Phys. B* **23**, 2846 (2009).